Imperial College London

100 years of living science

Medical Imaging

– Part II, towards real-time interactive and functional imaging

Professor Guang-Zhong Yang
Institute of Biomedical Engineering & Department of Computing

Cardiac Imaging Modalities

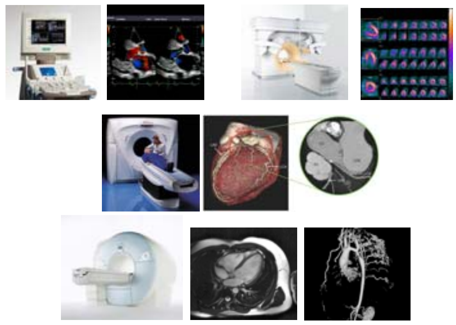

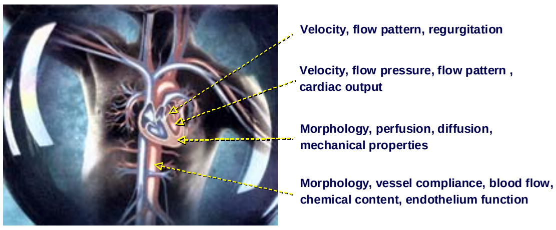

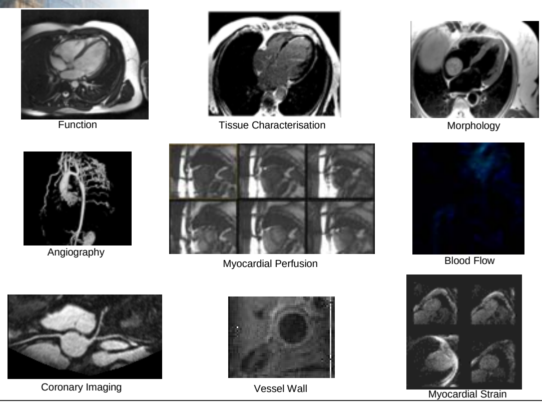

MRI Techniques for Myocardial Contractility

- MR tagging
- HARP - harmonic phase magnetic resonance imaging
- DENSE - displacement-encoded imaging with stimulated echoes
- Phase contrast myocardial velocity imaging

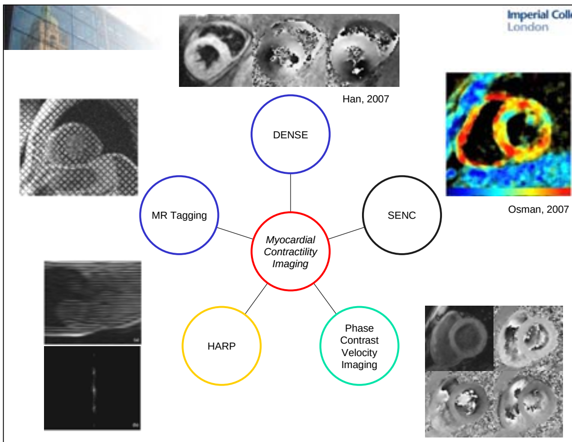

MR Tagging

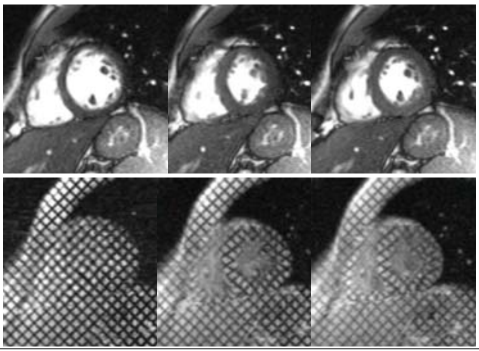

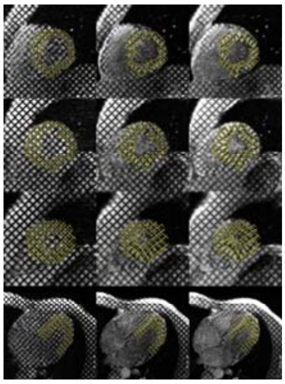

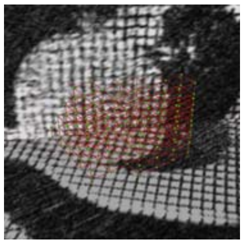

Raghavendra Chandrashekara

Tagging Analysis Techniques

Amini et al	radial+grid	2D ACM	thin-plate splines	motion simulator
Amini et al	grid	3D ACM	B-spline surfaces	motion simulator
Young et al	grid	3D ACM	finite-element model	gel phantom
Park et al	grid	3D ACM	deformable models	none
Kumar & Goldgof	grid	2D ACM	thin-plate splines	manual tracking
Guttman et al	radial & parallel	2D ACM/TM none		none

Active contour models (ACM), template matching (TM), optical flow (OF), harmonic phase (HARP).

Tagging Analysis Techniques

O'Dell et al	parallel	3D ACM/TM series expansion motion simulator
Declerck et al	parallel	3D ACM/TM planispheric transformation none
Denney & Prince	parallel	3D ACM/TM Fisher estimation motion simulator
Prince & McVeigh	grid	2D OF velocity fields motion simulator and phantom
Gupta & Prince	grid	2D OF velocity fields motion simulator
Dougherty et al	grid	2D OF velocity fields gel phantom
Osman et al	grid	2D – HARP motion simulator

Active contour models (ACM), template matching (TM), optical flow (OF), harmonic phase (HARP).

HARP MRI

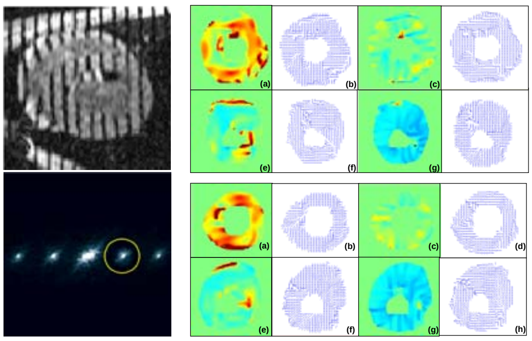

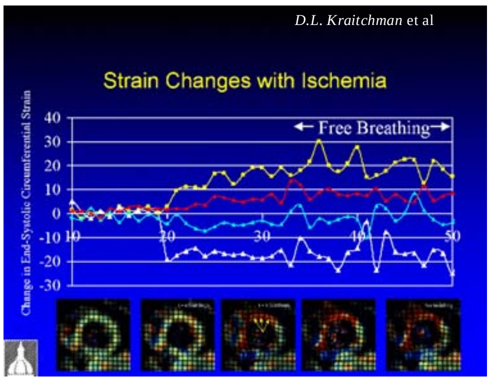

DENSE

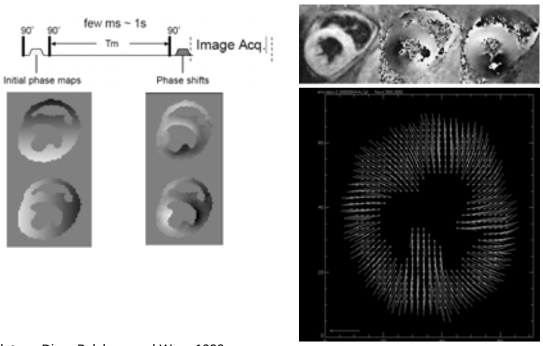

Aletras, Ding, Balaban, and Wen, 1999

MR Velocity Imaging

- Moran, PR (Magn Reson Imaging, 1982) - theory of phase velocity imaging
- Redpath TW, et al. (Phys Med Biol, 1984) & Feinberg DA, et al. (Magn Reson Med, 1985) - first Fourier velocity imaging
- van Dijk, P (J Comput Assist Tomogr, 1984) & Bryant DJ, et al. (J Comput Assist Tomogr, 1984) - First Phase mapping velocity images

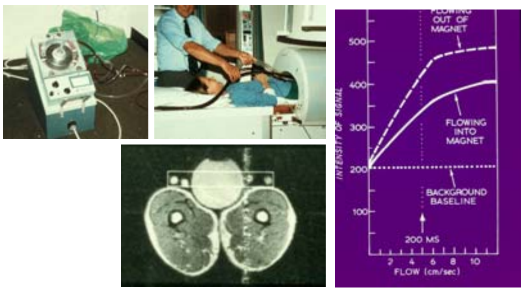

Saturation washin enhancement, 1982, Hammersmith, London

Phase Contrast Velocity Mapping

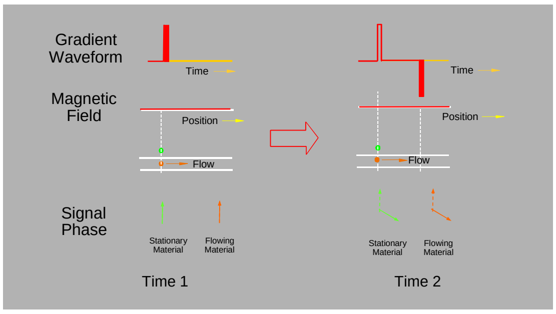

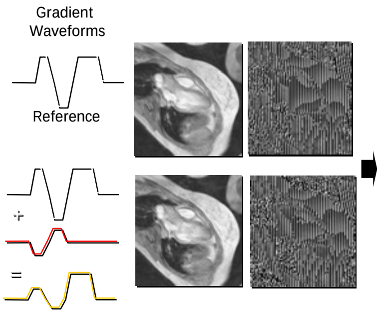

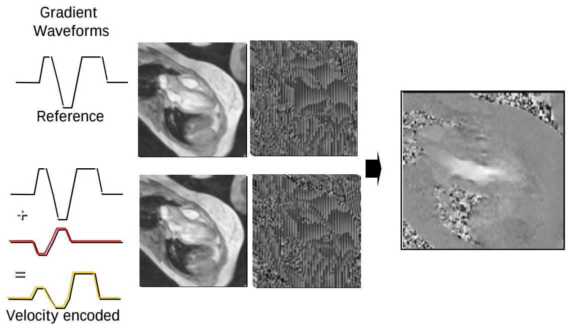

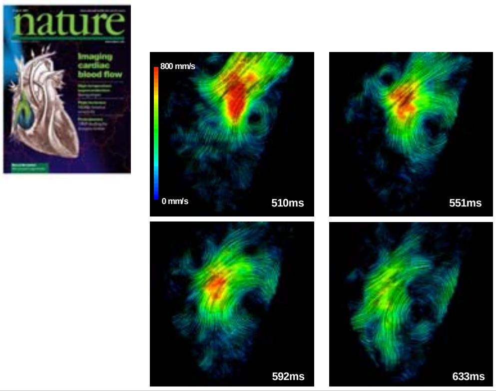

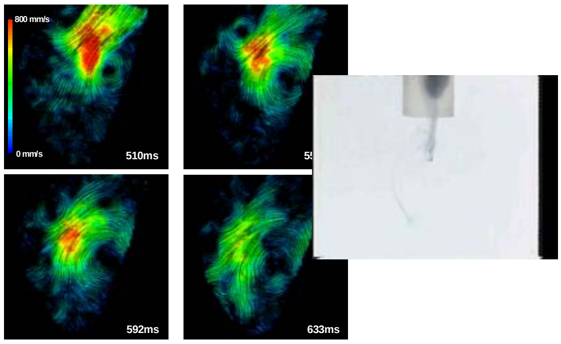

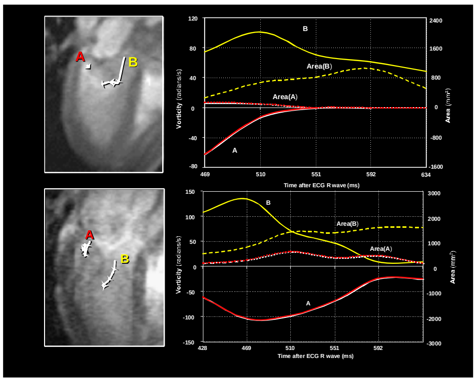

Myocardial Velocity Mapping

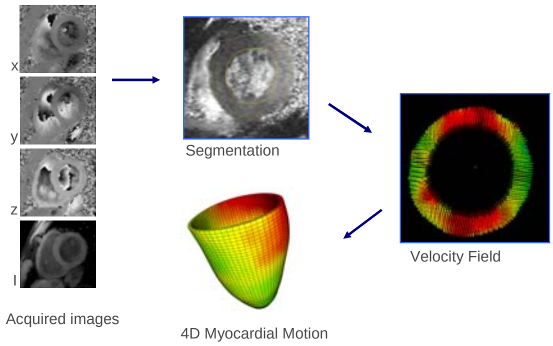

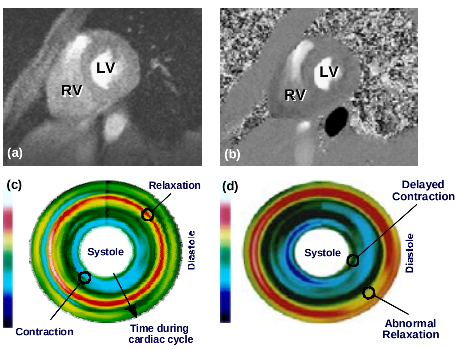

Technical Challenges

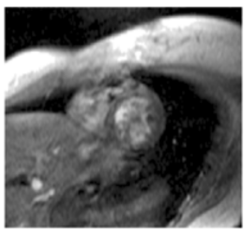

- Blood flow artefacts
- Low velocity sensitivity
- Low SNR

Presaturation Slab

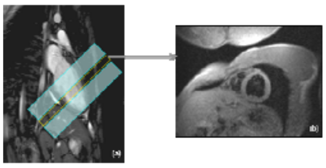

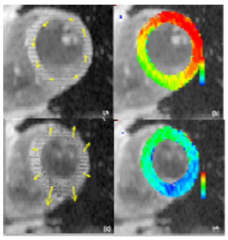

Reduces flow artefacts in the phase-encode direction

Computational Requirement

Preprocessing
- phase background correction
- phase unwrapping
- vector field restoration

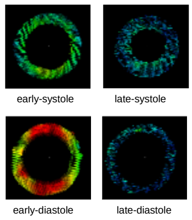

Contractility and modelling
- converting Eulerian velocity field to Lagrangian displacement (e.g. Fourier tracking, forward-backward integration)
- incorporating different regularization schemes (mainly geometrical, e.g. deformable mesh, spline models)
- incorporating biomechanical constraints (e.g., mass conservation, fibre-orientation) and the use of FEM

Computational Requirement

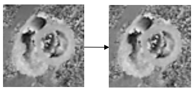

Preprocessing
- phase background correction
- phase unwrapping
- vector field restoration

Existing approaches
- Horn and Schunk, 1981 (optical flow with Euler-Lagrange)
- Song et al, 1993 (Poisson equation)
- Yang et al, 1993 (POCS)
- Buonocore, 1994 (divergence minimisation)
- Herment et al, 1999 (spatial regularization with diffusion process)
- Fatouraee & Amini, 2003 (divergence free & stream funciton)
- Ng and Yang 2003, Carmo & Yang, 2004 (total variation restoration)

Computational Requirement

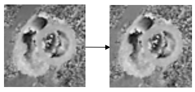

Preprocessing
- phase background correction
- phase unwrapping
- vector field restoration

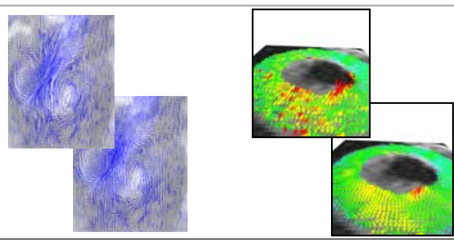

Total Variation Vector Restoration

- Removes noise in the velocity vector field
- Formulated as a constrained optimization problem

$$\text{Min} \quad E^{TV} = \sum_{\alpha}\left[\sum_{\beta\in N\alpha} d_l^2(u_\beta, u_\alpha)\right]^{\frac{1}{2}}$$

$$\text{Subject to} \quad h(u) = \frac{1}{2}\left[\sum_{\alpha} d_l^2(u_\alpha, u_\alpha^0) - |\Omega|\sigma^2\right] = 0$$

where **$d_l(f,g)$** is the embedded Euclidean distance between vectors f & g

Ω is the image domain,

σ^2 is the variance of the noise of the image,

u is the original image to be restored and,

u^0 is the noisy image

Total Variation Vector Restoration

Lagrangian function:

$$L(u;\lambda) = \sum_{\alpha}\left[\sum_{\beta\in N\alpha} d_l^2(u_\beta, u_\alpha)\right]^{\frac{1}{2}} + \frac{\lambda}{2}\left[\sum_{\alpha} d_l^2(u_\alpha, u_\alpha^0) - |\Omega|\sigma^2\right]$$

First order Lagrangian method:

$$u_\alpha^{n+1} = u_\alpha^n + \Delta t \cdot \prod\nolimits_{u\alpha}\left[\sum_{\beta\in N\alpha} wt_\alpha^\beta u_\beta + \lambda^n u_\alpha^0\right]$$

$$\lambda^{n+1} = \lambda^n + \Delta t \cdot \frac{1}{2}\left[\sum_{\alpha\in\Omega} d_l^2(u_\alpha, u_\alpha^0) - |\Omega|\sigma^2\right]$$

where

$$wt_\alpha^\beta = \left(\frac{1}{e(u;\alpha)} + \frac{1}{e(u;\beta)}\right)$$

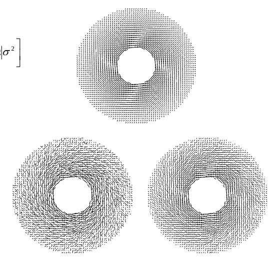

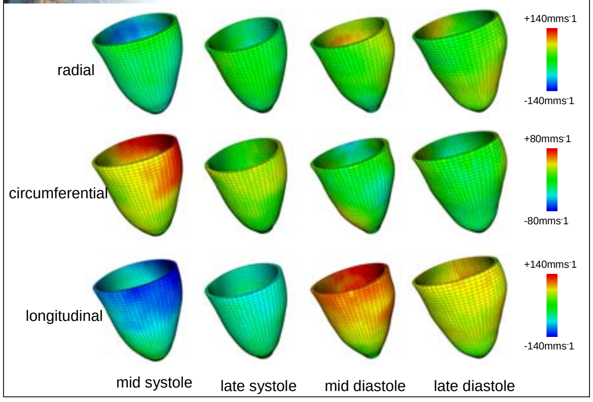

Computational Requirement

Preprocessing
- phase background correction
- phase unwrapping
- vector field restoration

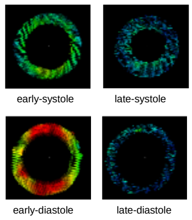

Contractility and modelling
- converting Eulerian velocity field to Lagrangian displacement (e.g. Fourier tracking, forward-backward integration)
- incorporating different regularization schemes (mainly geometrical, e.g. deformable mesh, spline models)
- incorporating biomechanical constraints (e.g., mass conservation, fibre-orientation) and the use of FEM

Computational Requirement

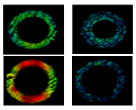

Contractility and modelling
- converting Eulerian velocity field to Lagrangian displacement (e.g. Fourier tracking, forward-backward integration)
- incorporating different regularization schemes (mainly geometrical, e.g. deformable mesh, spline models)
- incorporating biomechanical constraints (e.g., mass conservation, fibre-orientation) and the use of FEM

Existing approaches
- Young and Axel, 1992-1995 (model based approach and FEM)
- Van Wedeen, 1992 (strain rate tensor)
- Zhu, 1996, 1997, 1999 (Fourier tracking and saptio-temporal model)
- Meyer et al, 1996 (stochastic approach)
- Park et al, 1996 (volumetric deformable models)
- Amini et al, 1998 (coupled b-snake grids and constrained thin-plate splines)
- Arai et al 1999 (global local decoupled analysis)
- Masood et al 2002 (spline based virtual tagging)
- Chandrashekara and Rueckert, 2004 (spline based free form registration)
- Lee et al 2006, 2007 (FEM, Kriging and TV)

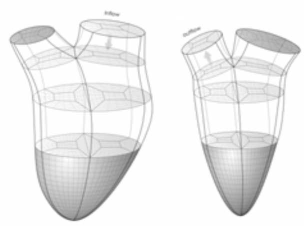

Lagrangian regularization (thin plate, Navier splines)

Statistical and spatio-temporal models

Physical based modelling (incorporating material property, anisotropic fibre orientation, and intra-ventricular pressure)

Semi-physical based modelling (e.g. virtual tagging incorporating mass conservation and the use of Kriging)

Coupled biomechanical and CFD modelling

Fibre Orientation

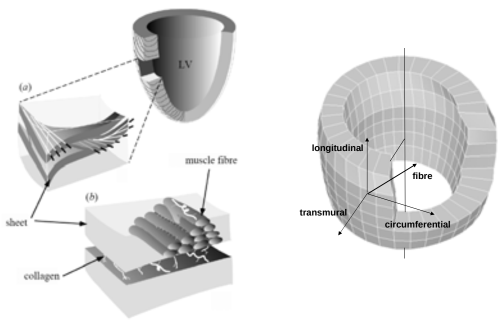

LeGrice, *et al.* 2001

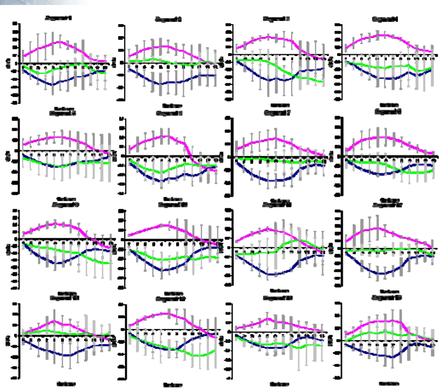

Biomechanical Analysis

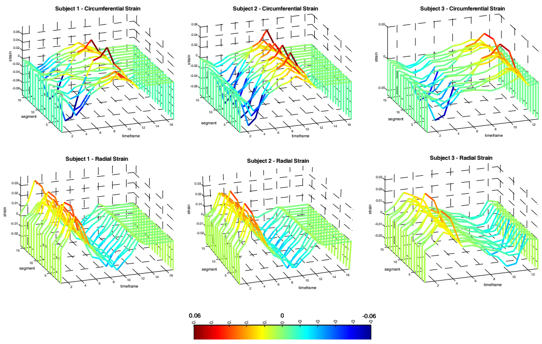

Coupled Biomechanical CFD Modelling

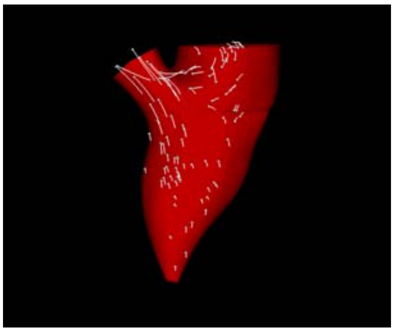

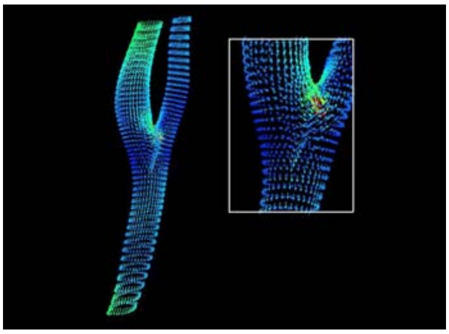

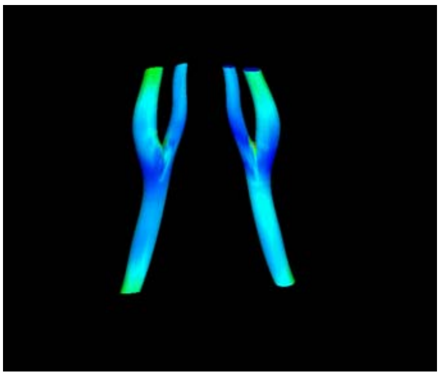

Valve Imaging

- Difficulty capturing valve leaflets
- Diastolic motion leads to underestimation of regurgitation*
- Ultrasound currently preferred

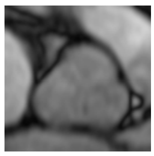

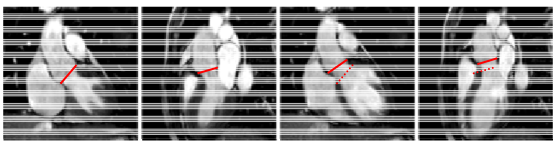

(a) End Systole (b) End Systole (a) End Diastole (b) End Diastole

* Kozerke *et al.*, J. Magn. Reson. Imaging, 14 (2001), 106-112

Ventricular Imaging

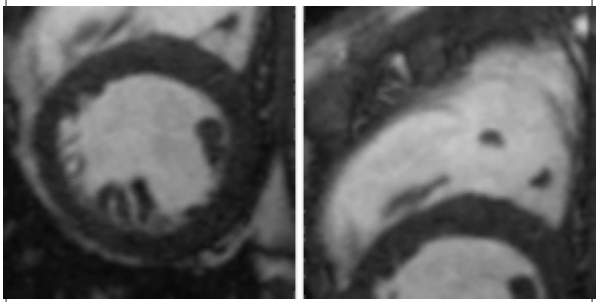

Left Ventricle | Right Ventricle

COMB Tagging

- Multiple parallel planes
- Can alter width and separation

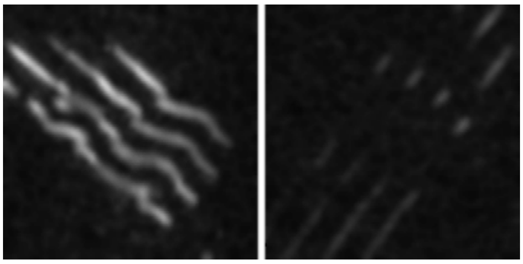

Horizontal Long Axis | Vertical Long Axis

Automated Tracking: To 3D

3D offset and orientation derived through the cardiac cycle

- Catmull-Rom Interpolation of 2D HLA/VLA tracking
- Orthogonal distance regression plane computed between tracked HLA/VLA myocardium

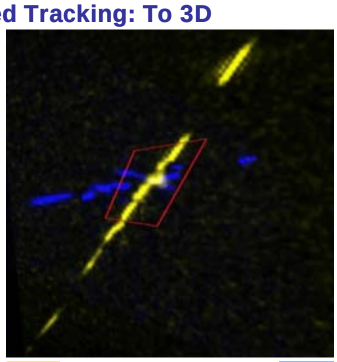

3D view of tracked tag

Adaptive Aortic Valve Imaging

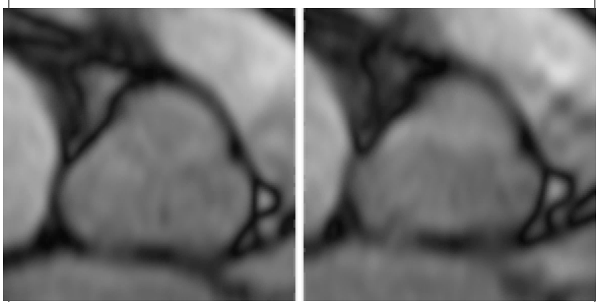

Conventional Imaging | Adaptive Imaging

Adaptive LV Imaging

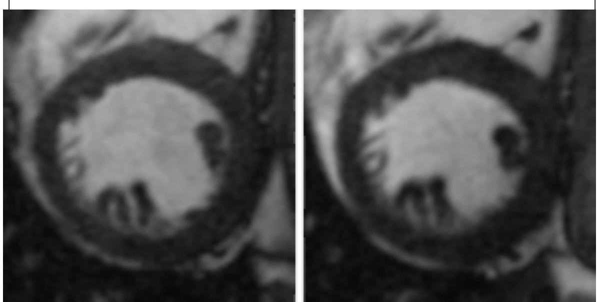

Conventional Imaging | Adaptive Imaging

Adaptive RV Imaging

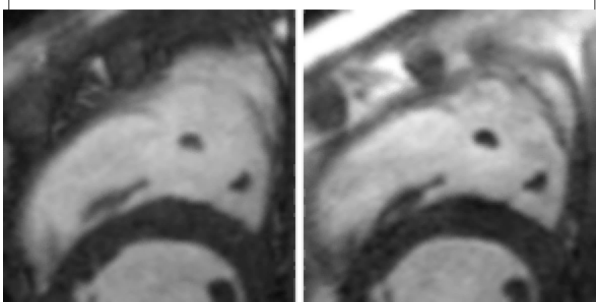

Conventional Imaging | Adaptive Imaging

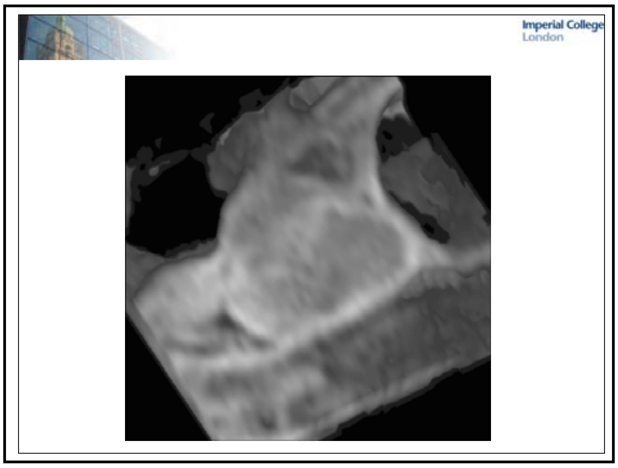

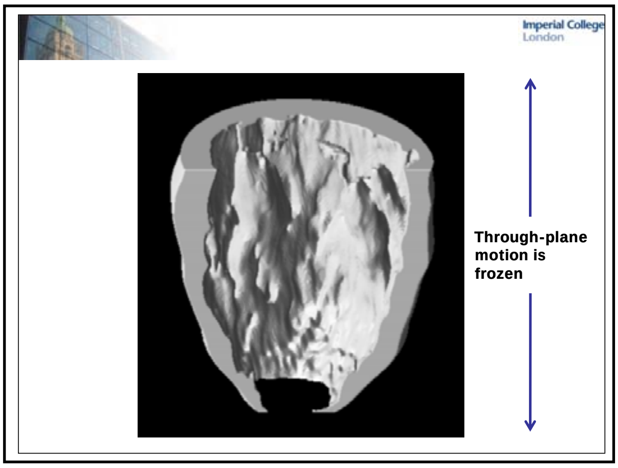
Through-plane motion is frozen


Through-plane motion is frozen
Radial Projection

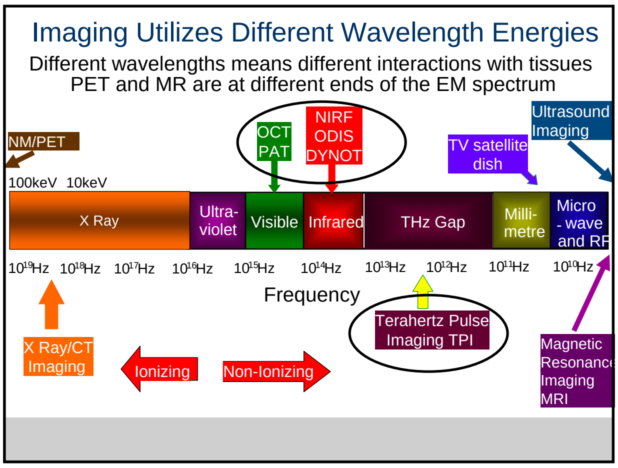
Imaging Utilizes Different Wavelength Energies
Different wavelengths means different interactions with tissues
PET and MR are at different ends of the EM spectrum
NM/PET
OCT PAT
NIRF ODIS DYNOT
TV satellite dish
Ultrasound Imaging
100keV 10keV
X Ray
Ultra-violet
Visible
Infrared
THz Gap
Milli-metre
Micro - wave and RF
10^19Hz 10^18Hz 10^17Hz 10^16Hz 10^15Hz 10^14Hz 10^13Hz 10^12Hz 10^11Hz 10^10Hz
Frequency
X Ray/CT Imaging
Ionizing
Non-Ionizing
Terahertz Pulse Imaging TPI
Magnetic Resonance Imaging MRI

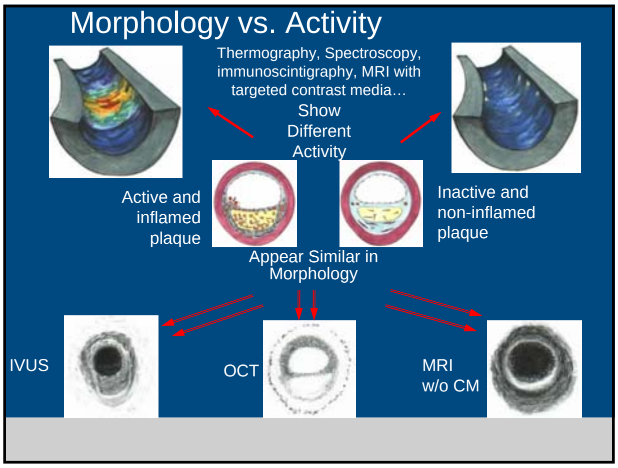
Morphology vs. Activity
Thermography, Spectroscopy, immunoscintigraphy, MRI with targeted contrast media…
Show Different Activity
Active and inflamed plaque
Inactive and non-inflamed plaque
Appear Similar in Morphology
IVUS
OCT
MRI w/o CM

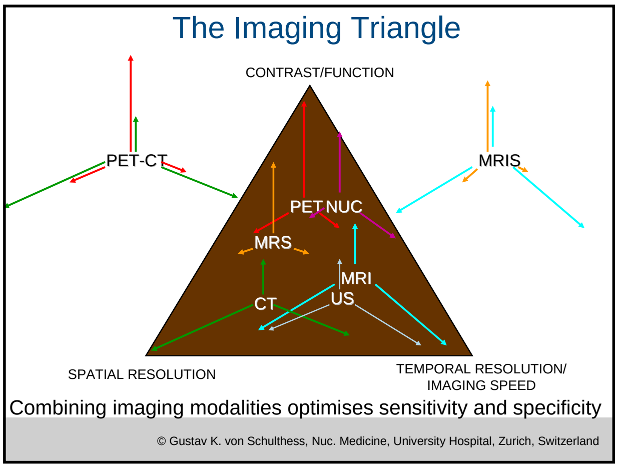
The Imaging Triangle
CONTRAST/FUNCTION
PET-CT
MRIS
PET NUC
MRS
MRI
CT
US
SPATIAL RESOLUTION
TEMPORAL RESOLUTION/ IMAGING SPEED
Combining imaging modalities optimises sensitivity and specificity
© Gustav K. von Schulthess, Nuc. Medicine, University Hospital, Zurich, Switzerland

PET/CT Cardiovascular Fusion

Courtesy of U Zurich, Switzerland

PET/CT Cardiovascular Fusion

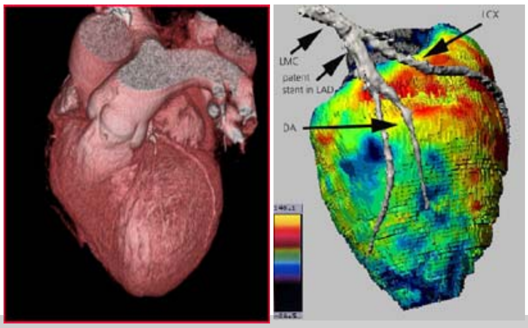

Courtesy of University Hospital Zurich, Switzerland

PET/CT Cardiovascular Fusion

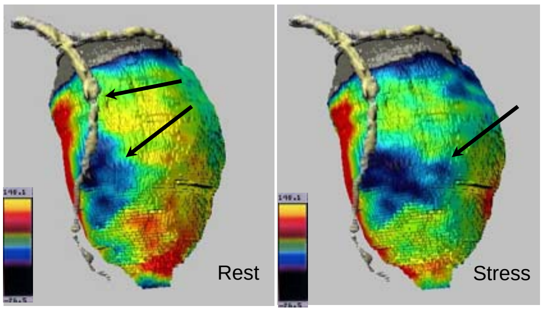

Courtesy of University Hospital Zurich, Switzerland

Uptake of ^{18}F-FDG in Symptomatic Plaque PET/CT Image Fusion

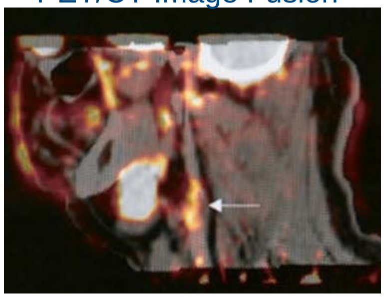

Uptake of ^{18}F-FDG is higher in inflamed carotid artery plaque and could be an indicator for plaque rupture

Rudd et al Cambridge University

MR Guided HI FUS

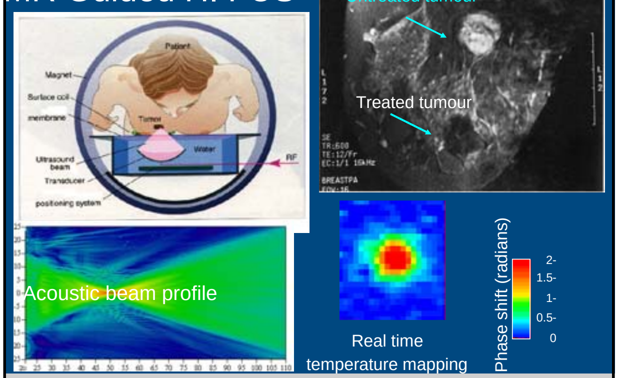

Guided Ultrasound Therapy

Encapsulated Drugs Released by Ultrasound at Disease Site

Ultrasound Hyperthermia

Destroy or Treat Disease Tissue

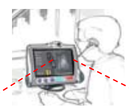

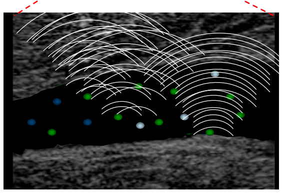

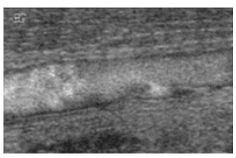

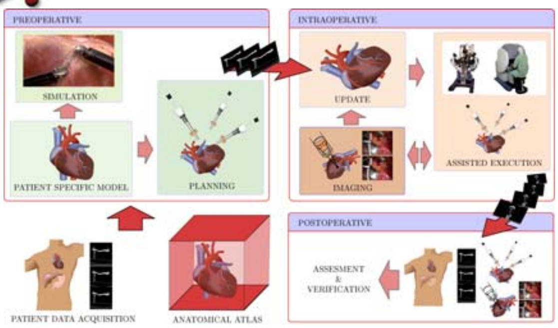

Reversal of Realism

pq-Space Representation

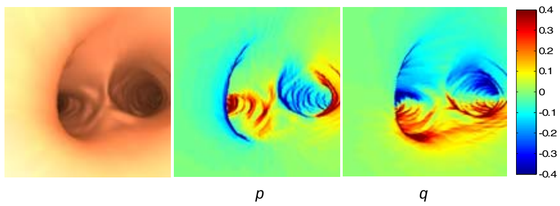

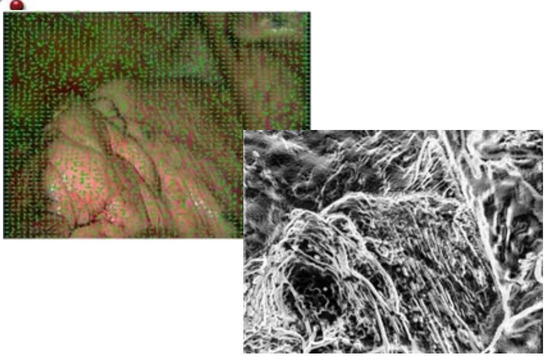

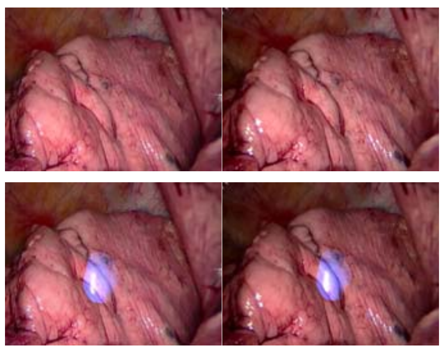

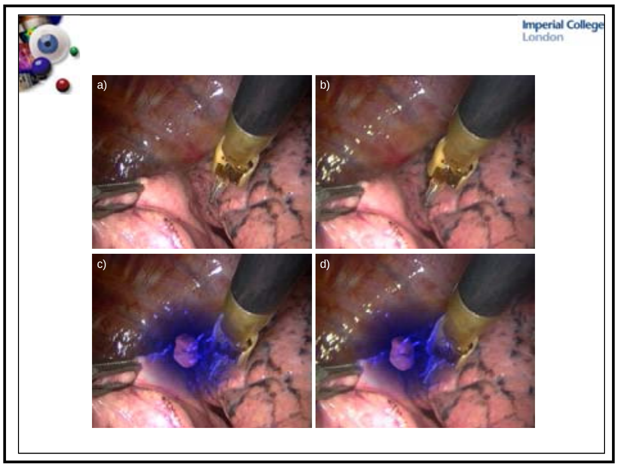
Imperial College
London
a)
b)
c)
d)

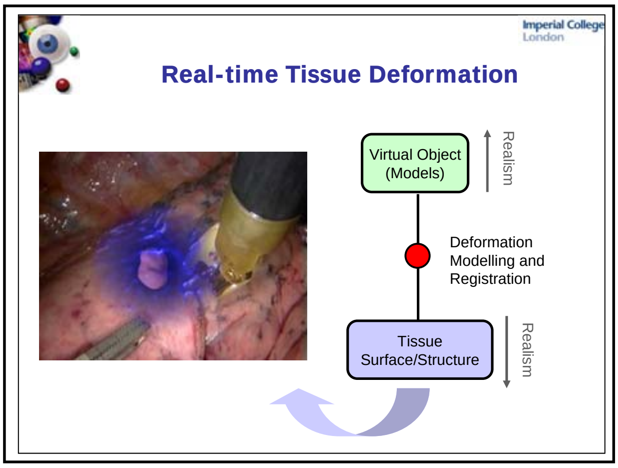
Imperial College
London
Real-time Tissue Deformation
Virtual Object
(Models)
Realism
Deformation
Modelling and
Registration
Tissue
Surface/Structure
Realism

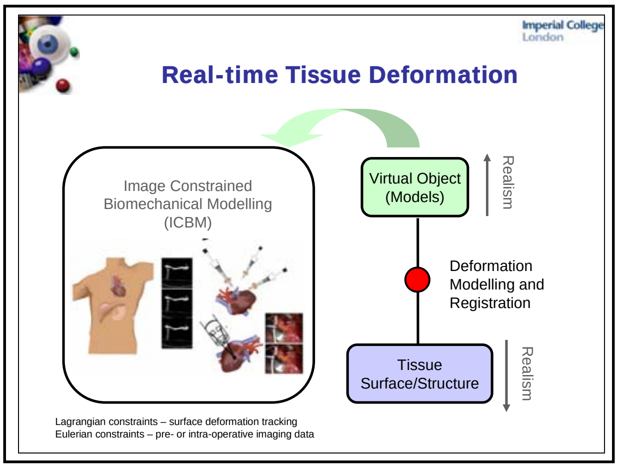
Imperial College
London
Real-time Tissue Deformation
Image Constrained
Biomechanical Modelling
(ICBM)
Virtual Object
(Models)
Realism
Deformation
Modelling and
Registration
Tissue
Surface/Structure
Realism
Lagrangian constraints – surface deformation tracking
Eulerian constraints – pre- or intra-operative imaging data

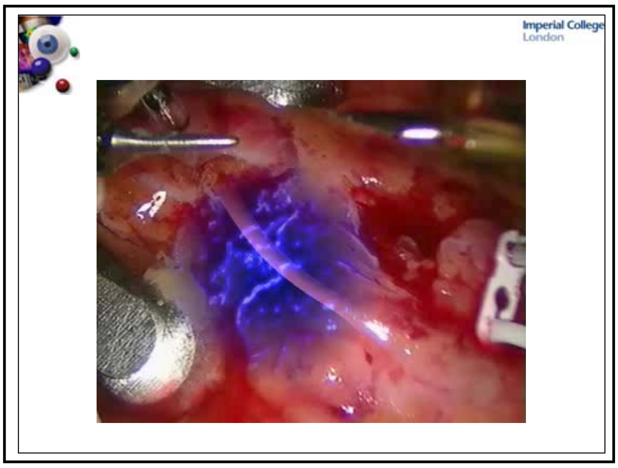
Imperial College
London

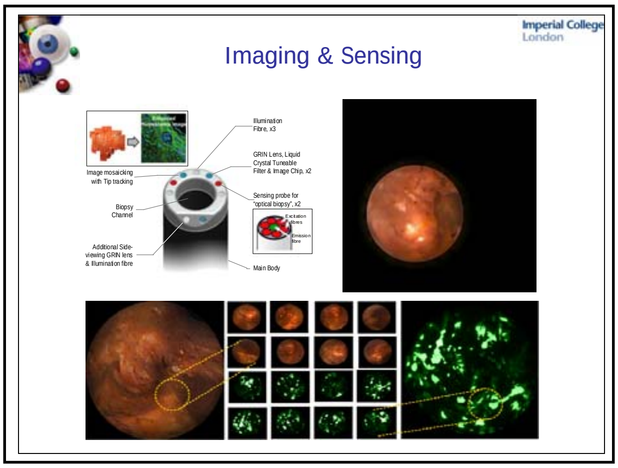
Imperial College
London
Imaging & Sensing
Illumination
Fibre, x3
GRIN Lens, Liquid
Crystal Tuneable
Filter & Image Chip, x2
Image mosaicking
with Tip tracking
Sensing probe for
"optical biopsy", x2
Biopsy
Channel
Excitation
fibres
Emission
fibre
Additional Side-
viewing GRIN lens
& Illumination fibre
Main Body

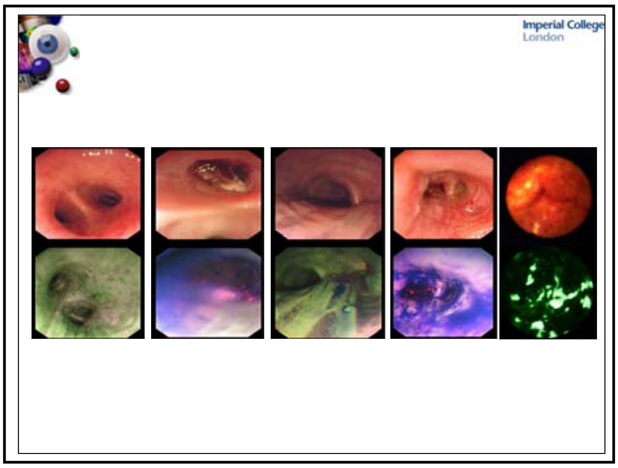
Imperial College
London

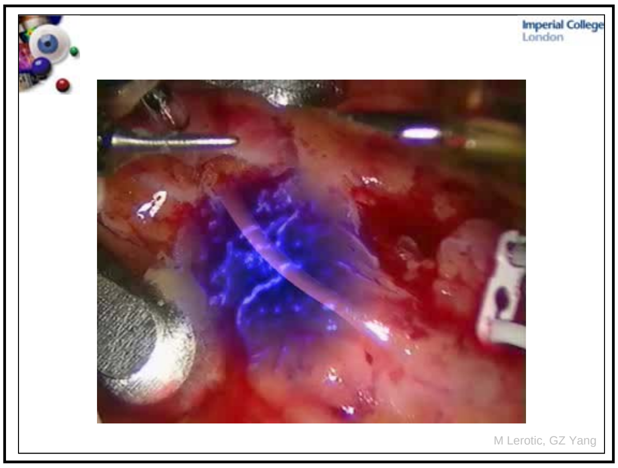
Imperial College London
M Lerotic, GZ Yang

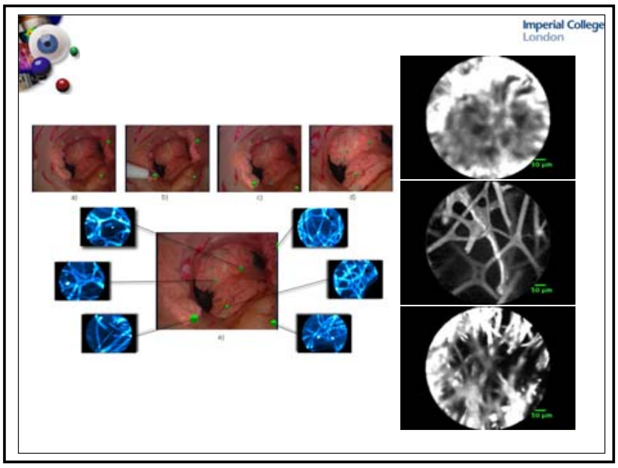
Imperial College London


c. 400 BC Disease concept introduced by Greek physician Hippocrates.
1612 Medical Thermometer devised by Italian physician Sanctorius
c. 1660 Light microscope developed by Dutch naturalist Antohj van Leeuwenhoek
1810 Stethoscope invented by French physician Rene' Laennec.
1850 - 1900 Germ theory of disease proposed by French scientist Louis Pasteur and developed by German bacteriologist Robert Koch.
1895 X-rays discovered by German physicist Wilhelm Conrad Roentgen. He also produced the first x-ray picture of the body (his wife's hand) in 1895.
1900 Chest x-ray, widespread use of the chest x-ray made early detection of tuberculosis (which was the most common cause of death) a reality.
1906 X-ray contrast medium. First contrast filled image of the renal system (kidneys).
1910 Barium sulfate introduction of as contrast agent for gastro-intestinal diagnosis.
1910-1912 Theory of Radioactivity published by Marie Curie and investigation of x-ray radiation for patient therapy (e.g. treatment of cancer).
1906 Electrocardiograph (ECG) invented by Dutch physiologist Willem Einthoven to monitor and record the electric signature of the heart.
1924 Radiographic imaging of the gallbladder, bile duct and blood vessels for the first time.
1929 Cardiac catheterization first performed by Forssmann on himself.
c. 1932 Transmission electron microscope (TEM) constructed by German scientists Max Knoll and Ernst Ruska.
1945 Coronary artery imaging. Visualization of (blood vessels that feed the heart).
1950 Nuclear Medicine applied imaging the kidneys, heart, and skeletal system.
1955 X-ray Image Intensifier-Television units to allow dynamic x-ray imaging of moving scenes. These fluoroscopic movies provided new information of the beating heart and its bloc
c. 1955 Panoramic x-ray images of the entire jaw and teeth.
1957 Fiber endoscopy pioneered by South African-born physician Basil Hirschowitz at the University of Michigan.
1960 Ultrasound imaging is developed to look at the abdomen and kidneys, fetal baby, carotid blood vessels and heart.
1970 X-ray mammography finds widespread application in imaging the breasts.
1972 Computed Tomography (CT) scanning invented by British engineer Godfrey Hounsfield of EMI Laboratories, England, and South African born physicist Allan Corn
1975 Chronic villus sampling developed by Chinese gynecologists as an aid to the early diagnosis of genetic disorders.
1976 Coronary Angioplasty was introduced by surgeon Andreas Gruentzig at the University Hospital, Zurich, Switzerland. This technique uses x-ray fluoroscopy to guide the compres
1978 Digital radiography: the TV signal from the x-ray system is converted to a digital picture which can then be enhanced for clearer diagnosis and stored digitally for future review.
1980 Magnetic Resonance Imaging (MRI) of the brain was first done on a clinical patient. MRI was developed by Paul Lauterbur and scientists at Thorn-EMI Laboratories
1984 3-Dimensional image processing using digital computers and CT or MR data, three dimensional images of bones and organs were first made.
1985 Clinical Positron Emission Tomography (PET) scanning developed by scientists at the University of California.
c. 1985 Clinical Networks were first implemented to allow digital diagnostic images to be shared between physicians via computer network, allowing a doctor in Boston to review a CT
1989 Spiral CT allows fast volume scanning of an entire organ during a single, short patient breath hold of 20 to 30 seconds. Spiral CT had caused a renaissance in CT and lead the
1989 MR Angiography developed and clinically available to allow non-invasive imaging of the blood vessels without radiation or contrast injection.
1993 Echo Planar MR Imaging (EPI) developed and clinically available to allow MR systems to provide early detection of acute stroke. EPI also makes possible functional imaging, f
1993 Open MRI Systems developed to allow MR scanning of severely claustrophobic or obese patients who could not tolerate convention MR imaging in a close bore system.

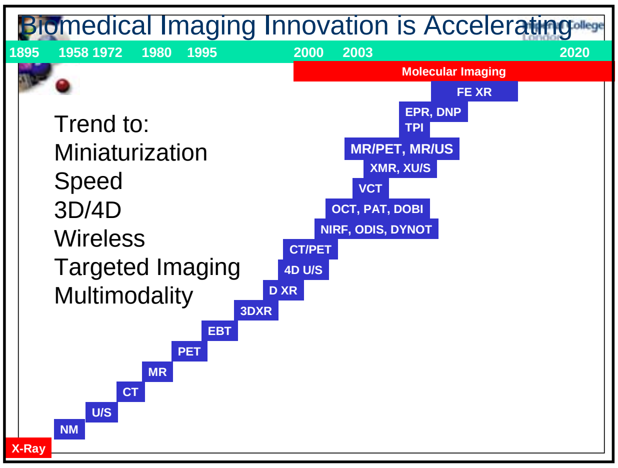
Biomedical Imaging Innovation is Accelerating
1895
1958 1972
1980
1995
2000
2003
2020
Molecular Imaging
Trend to:
Miniaturization
Speed
3D/4D
Wireless
Targeted Imaging
Multimodality
FE XR
EPR, DNP
TPI
MR/PET, MR/US
XMR, XU/S
VCT
OCT, PAT, DOBI
NIRF, ODIS, DYNOT
CT/PET
4D U/S
D XR
3DXR
EBT
PET
MR
CT
U/S
NM
X-Ray

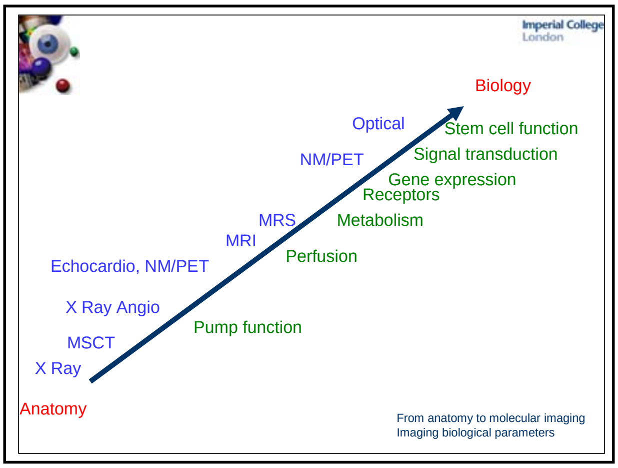
Imperial College London
Biology
Optical
Stem cell function
NM/PET
Signal transduction
Gene expression
Receptors
MRS
Metabolism
MRI
Echocardio, NM/PET
Perfusion
X Ray Angio
Pump function
MSCT
X Ray
Anatomy
From anatomy to molecular imaging
Imaging biological parameters

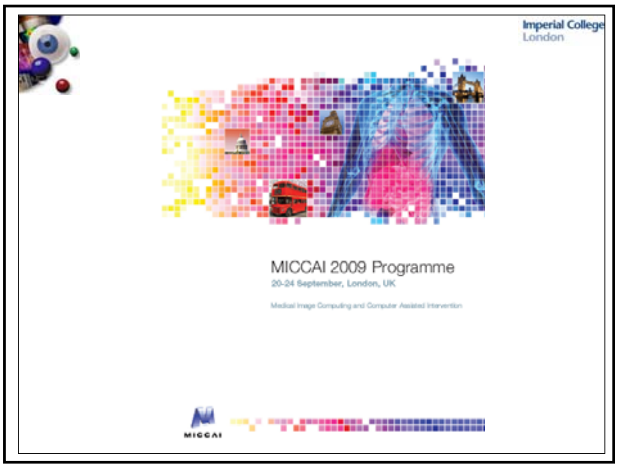
Imperial College London
MICCAI 2009 Programme
20-24 September, London, UK
Medical Image Computing and Computer Assisted Intervention
MICCAI